Synthesis of Bismuth Vanadate by a Novel Process and Its Enhanced Photoelectrochemical Performance

IOP Conf. Series: Materials Science and Engineering **562** (2019) 012097 doi:10.1088/1757-899X/562/1/012097

Synthesis of Bismuth Vanadate by a Novel Process and Its Enhanced Photoelectrochemical Performance

Fengkai Yu[1], Yan Zhang[1,*], Xiangzhong Ren[2], Meijun Yang[1] and Jianqiang Yu[1,*]

[1.] School of Chemistry and Chemical Engineering, Qingdao University, Qingdao 266071, China.
[2.] Jinan Institute of Chemical Engineering, Jinan 250000, China
Email: zhangyanchem@qdu.edu.cn, jianqyu@qdu.edu.cn

Abstract. Highly crystalline monoclinic scheelite $BiVO_4$ were synthesized by a hydrothermal process from strong redox reaction of VOC_2O_4 and $NaBiO_3$ solutions over a wide range of pH. A simple electrophoresis process was employed to fabricate the $BiVO_4$ thin films photoelectrochemical cell, which was used as photoanodes for water splitting. It can be found that the photoelectrochemical performance of the $BiVO_4$ thin-film is strongly dependent on the pH used in the synthesis. It demonstrated that the distortion and polarization of the local structure of the synthesized material dependent greatly on the pH condition during the synthesis. Moreover, upon pH=1, the photocurrent density increase. While the Flat band of these bismuth vanadate shifts to positive as the pH decrease, which means the Fermi Energy Level (E_f) is risen as the pH decrease, as well as the conductive band (CB). Electrochemical impedance spectroscopy (EIS) measurements suggested that the sample of pH=1 showed the highest rate of photogenerated charge transfer.

1. Introduction

Since photoelectrochemical water splitting was reported in 1972 [5], the development of *n*-type semiconductors that can serve as efficient photoanodes for solar water oxidation have attracted more and more attentions. *n*-type bismuth vanadate ($BiVO_4$) is one of the semiconductors [6]. It has been recently applied in many field, such as the water splitting [1, 2], CO_2 reduction [3], removal pollution [4]. $BiVO_4$ is a well-known photocatalytic material with a band gap nearly 2.4 eV and the appropriate valence band position for O_2 evolution [7, 8], outstanding light absorption edge up to 500 nm, and low cost of synthesis. Its conduction band located at ca. 2.4 V vs. RHE (reversible hydrogen electrode). However, its photocatalytic activity is usually low, because for water oxidation $BiVO_4$ suffer from excessive electron-hole recombination, poor charge transport properties. Some scientists have been focused on the synthesis method, which could enhance the activity of $BiVO_4$, such as morphology control [9]. Li *et al.* have investigated the activity of $BiVO_4$ with various facets [10], they find that the photogenerate electrons and holes occurred separately on the {010} and {110} facets under photo-irradiation.

In this study, we report a novel process for the synthesis of bismuth vanadate. The $BiVO_4$ was synthesized from aqueous VOC_2O_4 (Vanadyl oxalate) and $NaBiO_3$ (Sodium bismuthate dihydrate) solutions over a wide range of pH by a hydrothermal process. Vanadyl oxalate is organic vanadium source, the activity of organic compound is higher than that of inorganic compound. The $C_2O_4^{2-}$ (oxalic ion) shows a high reducibility, which can be easily oxidized to carbon dioxide. Therefore we selected bismuth(V) salt as the vanadium source. The carbon dioxide generate from the reaction may

increase the pressure of the reactor, and thus to make the $BiVO_4$ has a smaller particle size. The pH of the synthesis is also has a great role on the controlling of the morphology [10]. The electrochemical and photoelectrochemical properties were studied to understand the surface state and to evaluate the potential of the electrodes for PEC cell application.

2. Experiment

2.1. Materials

V_2O_5 (99 %, AR), $H_2C_2O_4{\cdot}2H_2O$ (99 %, AR), $NaBiO_3$ (99 %, AR), HNO_3 (69 %, AR), ammonium solution (28 %, AR), Platinum foil auxiliary and Ag/AgCl reference electrodes were purchased from Tianjin Aida Hengsheng Technology. Deionized water was made by the Flom ultrapure water system.

2.2. Preparation of Materials

VOC_2O_4 solution is prepared by dissolving V_2O_5 and $H_2C_2O_4$ ($M_{V_2O_5}: M_{H_2C_2O_4} = 1: 2.12$) in 100 ml deionized water, stiring under 50 °C for 2h. Then cold it down in temperature. It will be a transparent blue solution.

25ml above-mentioned VOC_2O_4 adjust various pH by adding 2 M HNO_3 and $NH_3{\cdot}H_2O$, reacting with 0.1 M $NaBiO_3$. Then put this solution in 100 ml PTFE (Polytetrafluoroethylene) reactor in 180 °C for 24h. The production washed by centrifugation.

$BiVO_4$ films were electrophoresised on a conductive FTO glass.

2.3. Characterization

X-ray diffraction (XRD) spectra were obtained on a DX-2700 X-ray diffractometer using Cu-Kα radiation over the range from 5˚ to 60˚. Scanning electron microscope (SEM) images were acquired on a JSM-6390F (JEOL, Tokyo, Japan) microscope by using an accelerating voltage of 20.0 kV. UV-visible diffuse reflectance spectra were obtained by a UV-vis diffuse reflectance spectrophotometer (U-41000. HITACHI, Tokyo, Japan). The photoelectrochemical measurements were carried out using a standard three-electrode cell and a electrochemical workstation (CompactStat.h10800).

3. Results and Discussion

3.1. Structure and Morphology of Material

To investigate the structure and morophology of $BiVO_4$, a variety of detection methods have been permormed.

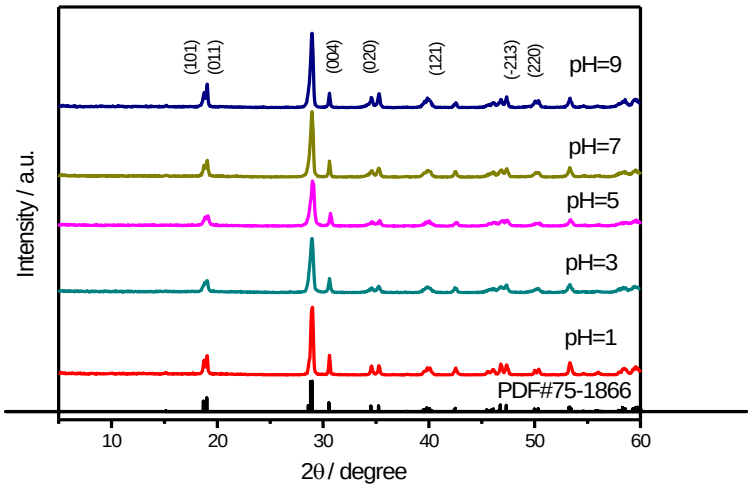

Figure 1. XRD patterns of products synthesized in different pH.

Fig. 1 shows X-ray diffraction patterns of samples synthesized in different pH. The peaks of 30.5, 35.2, 45.4, and 50.3˚ are observed corresponding to (004), (020), (-213) and (220) planes for the monoclinic phase of $BiVO_4$ (PDF#75-1866). That proved hydrothermal at 180 ˚C can make monoclinic phase of $BiVO_4$. The monoclinic $BiVO_4$ is known to show the highest photocatalytic effect than other crystal phases [11,12]. In the XRD, we can find the degree of crystallinity decreased firstly, and increase after pH5 as pH increased.

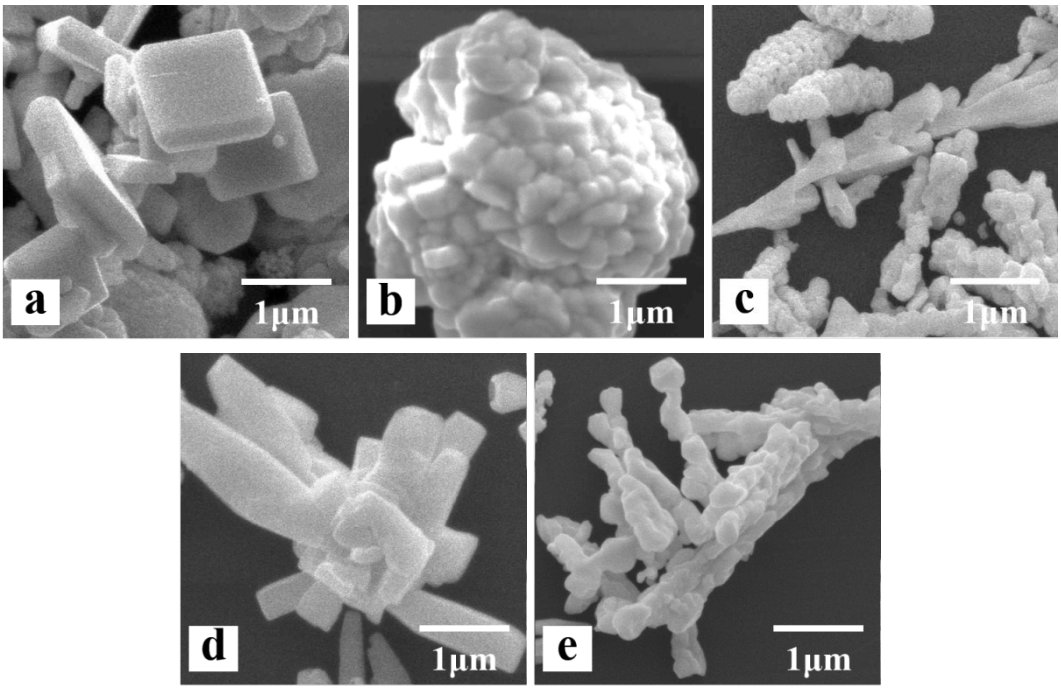

Figure 2. SEM images of products synthesized in different pH.
a. pH=1; b. pH=3; c. pH=5; d. pH=7; e. pH=9.

Fig. 2 presents scanning electron microscopy (SEM) images of samples. As shown in Fig. 2a, the sample (pH=1) powders show a morphology decahedron with the grain sizes of ca. 1 μm. The {010} and {110} facets separates obviously [10]. Compared with other samples, As the pH increase, morphology of $BiVO_4$ powders will change from sheet to rodlike grains. These long rods might be formed by the sintering of short rodlike grains in a one-dimensional fashion [9].

The UV-vis diffuse reflection spectra of samples were shown in Figure 3. The optical band gap was determined by the following equation (1):

$$\alpha h\nu = A(h\nu - E_g)^{\frac{n}{2}} \quad (1)$$

It was found that these samples displayed good photoabsorption properties ranging from ultraviolet to visible light with the wavelength shorter than 550 nm. There band gap energy is around 2.2eV.

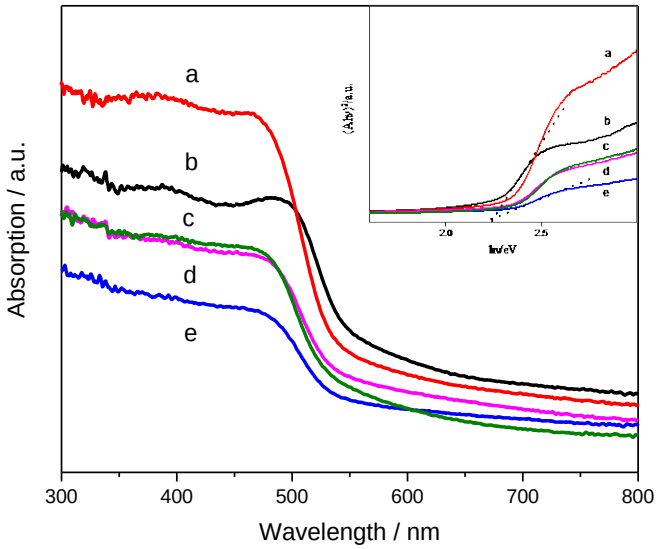

Figure 3. UV-vis images of products synthesized in different pH.
a. pH=1; b. pH=9; c. pH=7; d. pH=5; e. pH=3.

3.2. Photoelectrochemical Measurements

Photoelectrochemical measurements were used to tested the photoactivity of these films. A beam of visible light was irradiated on the back (FTO) side of the film immersed in 0.1 M NaOH (pH = 13). To converting the obtained potential (vs. Ag/AgCl) to RHE (NHE at pH = 0), the following equation (2) were used.

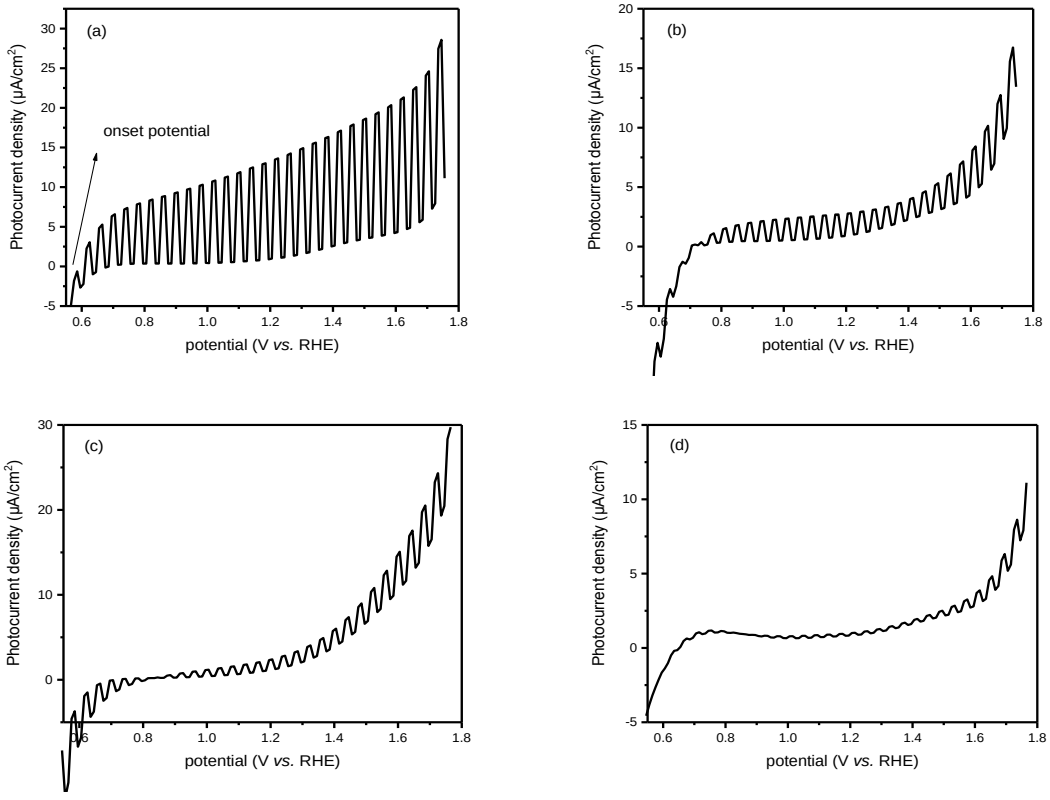

Figure 4. photocurrent–potential curves of samples.
a. pH=1; b. pH=3; c. pH=5; d. pH=7.

$$E_{RHE} = E_{Agcl} + 0.059\,pH + E^0_{Agcl} \quad (2)$$

Fig. 4 are the photocurrent–potential curves of $BiVO_4$ measured under visible light in 0.1 M NaOH. The photocurrents increased with increasing applied anodic potential representing a typical n-type semiconductor behaviour. Fig. 4 is a magnified view in 0.55–1.80 V (vs. RHE) of applied potentials to determine photocurrent onset potential. Onset potential is ca. (a) 0.55 V, (b) 0.7 V, (c) 0.8V, (d) 0.85V (vs. RHE). The onset potential shifted to negative potential by decreasing the synthesis pH. Thus, the fermi level is more positive with increasing of synthesis pH. The negative shift indicates there are larger accumulation of electrons in the $BiVO_4$ (pH=1) electrode and reflects decreased charge recombination [13]. However, due to the limitation of interfacial charge transport, we can't find precise value of flat band. So we test the Mott–Schottky plot.

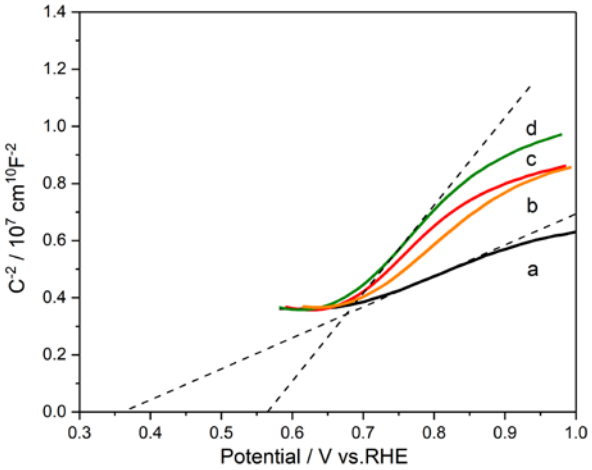

Figure 5. Mott–Schottky plot of samples.
a. pH=1; b. pH=3; c. pH=5; d. pH=7.

The flat band potential of electrodes can be determined by the Mott–Schottky curve used the following equation (3):

$$\frac{1}{C^2} = \frac{2}{e\varepsilon\varepsilon_0 N_D}\left(E - E_{fb} - \frac{\kappa T}{e}\right) \quad (3)$$

The value of the flat band potential of the thin-film synthesized at various pH can be calculated from **Fig. 5**. As we can find, the flat band potential of the sample synthesized at pH=1 is more negative than that of others. It demonstrated once again that we the dependence of flat band potential on the pH value used in the synthesis. Equation (3) also indicated that the slope is inversely proportional to the carrier concentration. Therefore, the carrier number in sample of pH=1 is higher.

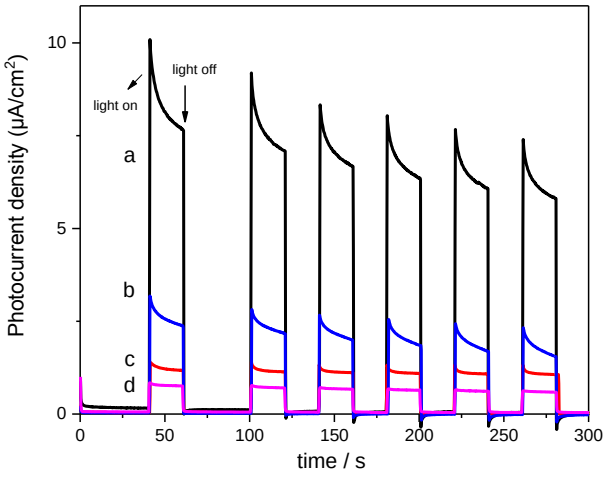

Figure 6. photocurrent density of samples.
a. pH=1; b. pH=3; c. pH=5; d. pH=7.

Fig. 6 indicates that the photocurrent density curves of the samples synthesized at various pH conditions. The photocurrent over the sample synthesized at pH=1 is the most intensive one. This result relates to the distortion and polarization of the material itself. As shown in Fig. 2, the morphology can be controlled by adjusting the synthesis pH condition. Thus, lower pH value will result in a larger distortion of Bi and V atoms in the local structure, the particle size decreases as well.

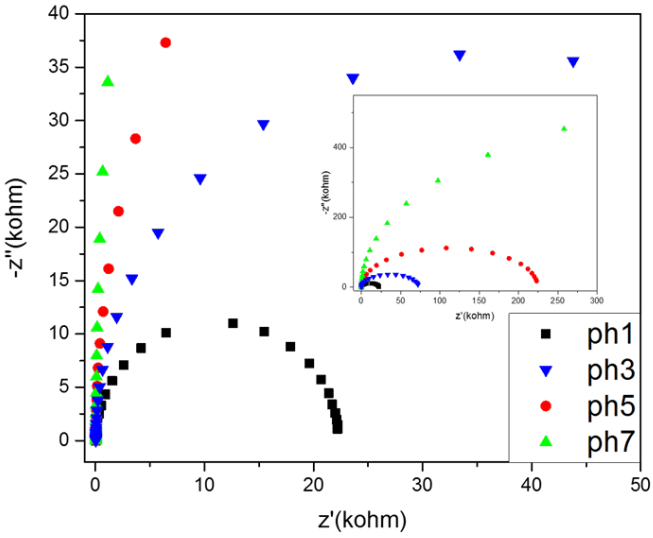

Figure 7. Nyquist plots of EIS.

The electrochemical impedance spectroscopy (EIS) measurements were performed to evaluate the kinetics of charge transfer. The EIS is a powerful tool to research electrochemical behaviour, especially the charge transfer at the photoanodes and water oxidation kinetics at the interface of the photoanode/electrolyte [13]. As shown in the Nyquist plots in Figure 7, the photoanodes show semicircles with different radii. The fitting of the semicircles indicate that samples synthesized in pH=1 has the lowest Rct. In contrast, when pH increases to 7, it shows the highest Rct. The reverse

tendency of the change in Rct from that of the PEC performance strongly suggests that synthesis pH is a critical factor in determining the photogenerated charge transfer of $BiVO_4$.

4. Conclusions

In summary, we investigated a novel process for the synthesis of bismuth vanadate from VOC_2O_4 and $NaBiO_3$ solutions by a hydrothermal process. Monoclinic $BiVO_4$ with various morphology can be synthesized by adjusting the pH condition. $BiVO_4$ sample synthesized at pH=1 shows the best photoelectrochemical water splitting performance. J-V plot suggests that $BiVO_4$ synthesized in pH=1 has a more negative onset potential, with a higher photocurrent. The EIS study demonstrated photogenerated charge transfer of pH=1 is the best, which were responsible for the distortion and polarization of the material itself.

5. References

[1] Kim, T. W.; Choi, K. S. 2014 *Science* **343** 990
[2] Murcialópez, S.; Fàbrega, C.; Monllorsatoca, D.; Hernándezalonso, M. D.; Penelaspérez, G.; Morata, A.; Morante, J. R.; Andreu, T. 2016 *ACS Appl. Mater. Interfaces* **8** 4076
[3] Liu, Y.; Huang, B.; Dai, Y.; Zhang, X.; Qin, X.; Jiang, M.; Whangbo, M. H. 2009 *Catal. Commun.* **11** 210-213
[4] Zhang, Y.; Yu, J.; Yu, D.; Zhou, X.; Lu, W. 2011 *Rare Metals* **30** 192-198
[5] Fujishima, A.; Honda, K. 1972 *Nature* **238** 37-38
[6] Kudo, A.; Omori, K.; Kato, H. 1999 *Cheminform* **121** 137-138
[7] Berglund, S. P.; Flaherty, D. W.; Hahn, N. T.; Bard, A. J.; Mullins, C. B. 2014 *J. Phys. Chem.C* **115** 3794-3802
[8] Iwase, A.; Kudo, A. 2010 *J. Mater. Chem.* **20** 7536-7542
[9] Yu, J.; Kudo, A. 2006 *Adv. Funct. Mater.* **16** 2163-2169
[10] Li, R.; Zhang, F.; Wang, D.; Yang, J.; Li, M.; Zhu, J.; Zhou, X.; Han, H.; Li, C. 2013 *Nat. Commun.* **4** 1432
[11] Kudo, A.; Omori, K.; Kato, H. 1999 *J. Am. Chem. Soc.* **121** 11459-11467
[12] Tokunaga, S.; Kato, H.; Kudo, A. 2001 *Chem. Mater.* **13** 4624-4628
[13] Hong, S. J.; Lee, S.; Jang, J. S.; Lee, J. S. 2001 *Energy & Environmental Science* **4** 1781-1787